Transp Porous Med (2011) 86:805–814
DOI 10.1007/s11242-010-9653-1

Experimental Study of Seepage Properties of Broken Sandstone Under Different Porosities

Xiexing Miao · Shuncai Li · Zhanqing Chen · Weiqun Liu

Received: 20 September 2009 / Accepted: 19 August 2010 / Published online: 4 September 2010

Abstract In coal mining the water flow in broken rock is a very common phenomenon. Study of seepage properties of broken rock is one of the basic subjects required in order to understand the stability of rock surrounding roadways, preventing disasters such as water inrush and gas outbursts and developing underground resources. So far, quantitative studies on the nonlinear seepage properties of broken sandstone under different porosities are not extensive in the research literature. In this article, by means of an electro-hydraulic servo-controlled test system (MTS815.02) and a patent seepage device, the seepage properties under different conditions of porosity were tested on broken sandstone of five different grain sizes. Based on the loading method of controlling the axial compression displacement and steady permeating method, we obtained curves of the relation of pore pressure with time, as well as the relation curves between the pore pressure gradient for steady seepage and velocity. Furthermore, we calculated the permeability k and non-Darcy coefficient β corresponding to different porosities by fitting these curves with the binomial expression. This study indicates that: (1) the seepage properties of broken sandstone are closely related to grain size, load levels, and porosity structure; (2) the permeability k decreases, while the coefficient β increases with a decrease in porosity φ, but both the $k - \varphi$ and the $\beta - \varphi$ curves show some local fluctuations; (3) the permeability k of the broken sandstone has a magnitude of 10^{-14}–10^{-12} m^2, while the coefficient β ranges from 10^{10} to 10^{12} m^{-1}. The results obtained provide some information for further study of the nonlinear seepage behavior of broken rock theoretically.

Keywords Broken sandstone · Steady seepage · Permeability · Non-Darcy coefficient β · Experimental study

X. Miao · Z. Chen · W. Liu
State Key Laboratory for Geomechanics and Deep Underground Engineering, China University of Mining and Technology, Xuzhou 221008, Jiangsu, China

S. Li (✉)
School of Mechanical and Electrical Engineering, Xuzhou Normal University, Xuzhou 221116, Jiangsu, China
e-mail: zsclsc@263.net

1 Introduction

Broken rock from coal mining can be classified into two kinds (Liu 2002): the first one is called the original-position broken rock which stays in its original position after it is broken by primitive structural and mining stresses; the other one is called the piled broken rock which is accumulated from the collapsed broken rock. The seepage properties of these two kinds of broken rock are markedly different from those of pore structural rock or fractured rock and their permeability is much larger than that of pore structural rock. Due to this high permeability, flow catastrophes and water inrush accidents are apt to take place in the broken zones of aquifers. Investigators such as Kogure (1976), Zoback and Byerlee (1976), McCorquodale et al. (1978), Pradip Kumar and Venkataraman (1995), Wang et al. (1996), Legrand (2002), Engelhardt and Finsterle (2003), and others have carried out many experiments on the flow in broken rock. In particular, Stephson (1984) summarized the experimental results of flow in rock fills and concluded that the Reynolds number Re in laboratory tests is far lower than that in in-situ tests. When Re is larger than 10^4, the hydraulic gradient J is proportional to the square of the flow velocity$v$and when Re is less than 10^4, J is proportional to $v^{1.85}$. Li et al. (1998) obtained the theoretical relations between the frictional coefficient, Re, J, and flow velocity v. For many years, in order to find a general equation that would fit most of the available experimental data, many extensions of Darcy's law have been proposed and many investigators developed formulas for non-Darcy flows in rock fills by theoretical or empirical methods, of which the following three are but examples (Bear 1979; Irmay 1958; Giorgi 1997)

$$J = Av + Bv^2 \tag{1}$$

$$J = Av + Bv^2 + C\frac{\partial v}{\partial t} \tag{2}$$

$$-\nabla p = \mu k^{-1}\vec{v} + \rho\beta\,|\vec{v}|\,\vec{v} \tag{3}$$

where A, B, and C are the coefficients relating to block shape, size, porosity and fluid properties. Δp is pore pressure gradient, k is the permeability of the rock fills, $\vec{v}$ is the vector of flow velocity, ρ, μ are, respectively, the mass density and dynamic viscosity of the fluid, β is non-Darcy coefficient and when the non-Darcy coefficient β obtained from the experiment is close to zero, the flow satisfies the Darcy law.

Liu and Miao (2003) and Ma (2003) studied the seepage properties of broken shale, sandstone, and coal under different stress levels; however, they did not provide quantitative rules of the seepage properties of non-Darcy flows in relation to porosity. In our study, we have analyzed qualitatively and quantitatively seepage properties of broken sandstone of different grain sizes under different axial displacements (or different porosities). The results obtained can provide some information for further study of the seepage behavior of broken rock.

2 Test Principle and Method

The test on seepage properties of broken sandstone was carried out by an electro-hydraulic servo-controlled test system (MTS815.02) and a patent seepage device for broken rock (Li 2006) as shown in Fig. 1. The broken rock was placed in the cylinder tank. The testing of the sandstone core confirmed that its uniaxial compressive strength was 57.5 MPa and density 2473 kg/m^3. Before the experiments, the sandstone needed to be broken and classified into different grain sizes, i.e., diameters. We used a grading sieve to select four basic grain sizes and a mixed fifth grain size: No. 1: 5–10 mm, No. 2: 10–15 mm, No. 3: 15–20 mm, No. 4:

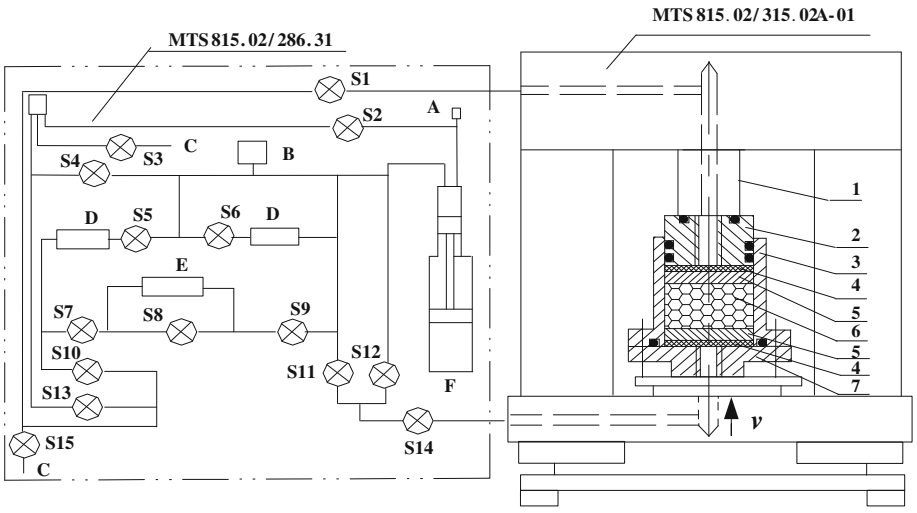

Fig. 1 MTS 815.02 rock test and seepage systems. Note: A–pressure transducer; B–pressure relief valve; C–drainage; D–stabilizer; E–differential pressure transducer; F–pressure intensifier (booster); S1–S15 are switches. 1–spherically seated upper platen for axial loading; 2–piston; 3–cylinder tank; 4–felt; 5–permeable plate with many holes; 6–rock sample; 7–base plate

20–25 mm and No. 5: mixed grain (composed of the four grain diameters with a mass ratio of 1:1:1:1).

The above test system (MTS 815.02) contains two subsystems: 315.02A-01 axial load system and 286.31 pore water pressure load system. We used a loading method of controlling the axial displacement, which included four to six levels: 10, 20, 25, 30, 35, and 40 mm. After each axial displacement has been loaded, the system can hold this displacement, and pore pressure system begins to load, namely, pressure intensifier piston begins to shift according to the pre-designed velocity. As in this system the maximum displacement of the pressure intensifier piston is 100 mm, its velocity v_1 was set at four rates: 10, 20, 30, and 40 mm/min. In order to avoid a sharp increase in pore pressure at the last displacement level, the corresponding velocity v_1 needed to be decreased gradually. Accordingly, flow velocity v can be calculated by the velocity v_1 of the pressure intensifier piston according to the condition that the flowrate Q (where $Q = \mathrm{A}v$) through the intensifier and the permeable plate is equal. With a diameter of the intensifier piston 5.5 cm and the inner diameter of the cylinder tank 12.7 cm (the diameter of permeable plate is also 12.7 cm), we obtained flow velocity v

$$v = \left(\frac{5.5}{12.7}\right)^2 v_1 \tag{4}$$

As mentioned above, axial displacement S and piston velocity v_1 of the pressure intensifier can be pre-designed by software of MTS815.02 system, and at each level of axial displacement (thus, at this time the total height H_s of the sample is also kept unchanged), we designed the four fixed flow velocities v.

The porosity φ of each displacement level can be developed as follows

$$\varphi = 1 - \frac{m}{\rho_\mathrm{s} A(H_0 - S)} \tag{5}$$

where m, ρ_s, H_0 are the mass, mass density, and the initial height of the broken sample, respectively, A the cross section area of the cylinder tank.

In Fig. 1, the one-dimensional seepage direction x is vertical upward. When the flow is steady, according to the Eq. 3, we use the Forchheimer equation to express the relation of pressure gradient and flow velocity

$$-\frac{\partial p}{\partial x} = \frac{\mu}{k}v + \rho\beta v^2 \tag{6}$$

The reason for using the law of non-Darcy flow is as follows: for the porous media, Reynolds number Re is defined as

$$Re = \frac{\rho v d}{\varphi\mu} \tag{7}$$

where d is the average diameter of the grains for the non-consolidated porous media. The earlier research indicated that the upper limit of Re suitable for Darcy law is five Kong (1999) and for different media this limit is slightly different.

According to Eq. 4, in our test, $v_{\min} = 3.13 \times 10^{-5}$m/s, $v_{\max} = 7.50 \times 10^{-5}$m/s. Taking $d = 10$–25 mm, $\varphi = 0.48$–0.19, $\rho = 1000\,\mathrm{kg/m^3}$ and $\mu = 1.01 \times 10^{-3}$ Pa.s into Eq. 7, we have

$$Re = \frac{\rho v d}{\varphi\mu} = 0.645\text{–}9.773$$

So, it is possible that Re is greater than five and non-Darcy flow follows. In order to fully consider the possibility of non-Darcy flow existing, we used the experimental data to plot the relation curves between $\frac{\partial p}{\partial x}$ and v, from which we can judge the changing of the seepage flow form.

The first purpose of our test is to obtain the steady pore pressure corresponding to each flow velocity v. In the test, the upstream end of the rock sample was connected to the pressure intensifier tank of the test system, which could automatically record the changing pore water pressure p over time t, and here, we assume that p_1 is the steady value of p at the intake boundary, while the downstream end was connected with atmosphere resulting in a pore water pressure p_2 of zero. In our experiments, flow velocity is fixed; and if p is steady then the flow in sample is also steady and in the same time the height of sample is kept invariable at the stage of seepage, so the pore pressure gradient is also steady.

Next, we will develop the calculation of steady pore pressure gradient. Conditioned that all the parameters of the right side in the Eq. 6 do not change with x, then pore pressure gradient $\frac{\partial p}{\partial x}$ is a constant and can be determined by the pore pressure at the two ends of sample and then we can get

$$\frac{\partial p}{\partial x} = \frac{p_2 - p_1}{H_s} = -\frac{p_1}{H_s} \tag{8}$$

where H_s is the height of the broken sandstone, and $H_s = H_0 - S$.

In our experiment, the total height of sample is only 10 cm and it is nearly impossible to precisely measure the parameters of pore structure in range of each 1 cm, so we assumed that the overall body porosity φ of sample could represent its average, and parameters k, β and v were all the averages in sample. For this reason, we made the sample distribute as uniformly as possible when filling grains and reduced at best the fluctuation of the above parameters with x. So, when flow is steady, the pore pressure gradient corresponding to each seepage flow velocity v can be calculated by Eq. 8.

According to each flow velocity $v$and the steady value of $\frac{\partial p}{\partial x}$, we can draw the $(\frac{\partial p}{\partial x}, v)$ scatter diagram. From the regression of $\frac{\partial p}{\partial x}$ as a function of v by Eq. 6, we can calculate the permeability k and the non-Darcy coefficient β at each porosity level.

3 Test Results

For the broken sandstone with a 5–10 mm grain diameter, the curves of pore pressure p changing over time t at various axial displacements can be obtained. As shown in Fig. 2, we have given the curves of p changing with t corresponding to the four velocities v_1 at axial displacement 10, 15, 20, and 25 mm, respectively.

From these curves the steady pressure p_1 can be obtained, then by Eqs. 4 and 8, flow velocity and pressure gradient at each axial displacement level are listed in Table 1.

From Table 1, the relationships between pore pressure gradient and flow velocity at various axial displacements S for 5–10 mm sandstone are presented in Fig. 3.

By fitting all the curves in Fig. 3 with Eq. 6, the permeability k and non-Darcy coefficient β at various porosities φ can be calculated as shown in Table 2.

Accordingly, by Table 2 the curves of k and β changing with porosity φ for 5–10 mm broken sandstone are presented in Fig. 4.

Similarly, the curves of $k-\varphi$ and $\beta-\varphi$ for the other four grain sizes of broken sandstone are given as shown in (a), (b), (c), and (d) of Fig. 5, respectively.

In order to compare the seepage properties of these five different sizes of broken sandstone, curves of the permeability k and non-Darcy coefficient β varying with porosity φ are presented in (a) and (b) of Fig. 6, respectively.

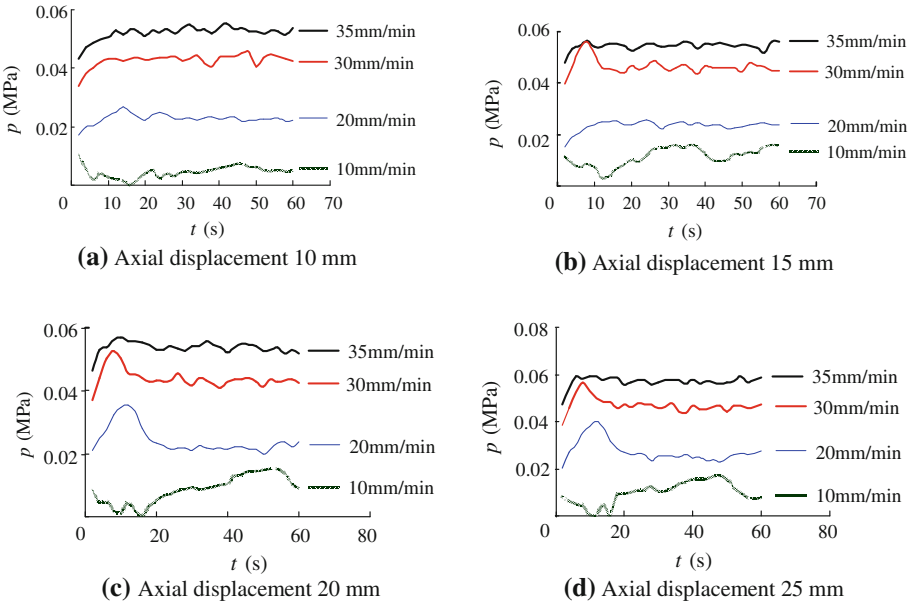

Fig. 2 Curves of pore pressures changing with time at each axial displacement for 5–10 mm sandstone

Table 1 Pressure gradient and flow velocity at each axial displacement level for 5–10 mm sandstone

Axial displacement S (mm)	Height H_S (mm)	Porosity φ	Piston velocity v_1 (mm/min)	Flow velocity v (mm/s)	Pressure gradient $\frac{\partial p}{\partial x}$ (MPa/mm)
10	100	0.4573	10	3.13×10^{-2}	-5.05×10^{-5}
			20	6.25×10^{-2}	-2.29×10^{-4}
			30	9.38×10^{-2}	-4.33×10^{-4}
			35	1.09×10^{-1}	-5.29×10^{-4}
15	95	0.4287	10	3.13×10^{-2}	-1.40×10^{-4}
			20	6.25×10^{-2}	-2.52×10^{-4}
			30	9.38×10^{-2}	-4.85×10^{-4}
			35	1.09×10^{-1}	-5.76×10^{-4}
20	90	0.3970	10	3.13×10^{-2}	-1.32×10^{-4}
			20	6.25×10^{-2}	-2.44×10^{-4}
			30	9.38×10^{-2}	-4.78×10^{-4}
			35	1.09×10^{-1}	-5.95×10^{-4}
25	85	0.3615	10	3.13×10^{-2}	-1.43×10^{-4}
			20	6.25×10^{-2}	-2.99×10^{-4}
			30	9.38×10^{-2}	-5.44×10^{-4}
			35	1.09×10^{-1}	-6.71×10^{-4}
30	80	0.3216	10	3.13×10^{-2}	-3.07×10^{-4}
			20	6.25×10^{-2}	-5.17×10^{-4}
			30	9.38×10^{-2}	-8.20×10^{-4}
			35	1.09×10^{-1}	-9.73×10^{-4}
35	75	0.2764	10	3.13×10^{-2}	-5.28×10^{-4}
			20	6.25×10^{-2}	-1.08×10^{-3}
			30	9.38×10^{-2}	-1.65×10^{-3}
			35	1.09×10^{-1}	-2.07×10^{-3}
40	70	0.2247	6	1.88×10^{-2}	-1.19×10^{-3}
			12	3.75×10^{-2}	-2.20×10^{-3}
			18	5.63×10^{-2}	-3.22×10^{-3}
			21	6.56×10^{-2}	-5.23×10^{-3}

4 Analyses of Test Results

Given the curves presented above, we can observe the following rules:

(1) As shown in Fig. 2, about 15–20 s is required to attain to a steady state of seepage for each flow. At each axial displacement level, the stability of the pore water pressure corresponding to the first velocity is comparatively weak, because the sample had just undergone the earlier axial deformation and its pore structure was being adjusted locally.

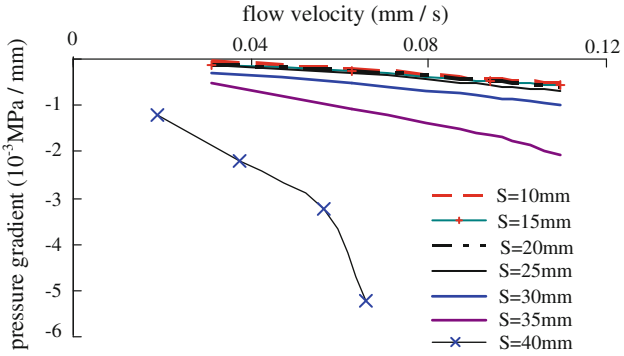

Fig. 3 $\frac{\partial p}{\partial x} - v$ curves at different displacements for 5–10 mm sandstone

Table 2 Seepage properties under different porosities for 5–10 mm sandstone

S (mm)	10	15	20	25	30	35	40
φ	0.4573	0.4287	0.3970	0.3615	0.3216	0.2764	0.2247
k (10^{-13} m^2)	7.21	3.16	3.74	2.97	1.17	0.064	0.281
β (10^{10} m^{-1})	3.24	1.89	2.49	2.51	0.19	3.18	57.2

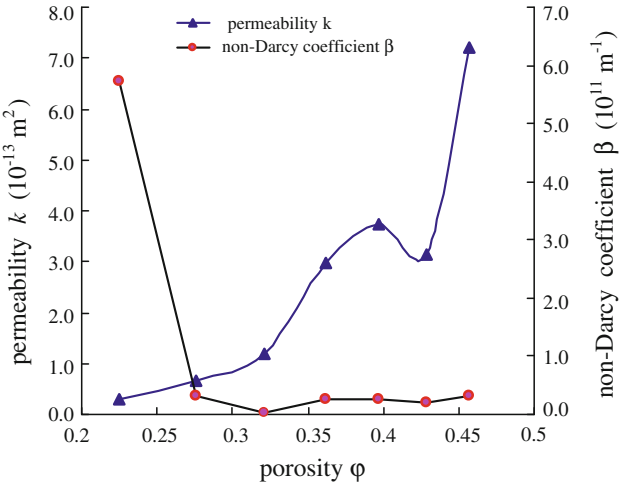

Fig. 4 $k - \varphi$ and $\beta - \varphi$ curves for 5–10 mm sandstone

(2) From Figs. 4–5, it is seen that during the axial compression, the permeability k decreases while the absolute value of coefficient β increases with the decreasing of porosity φ except some local fluctuations (there is an exception in Fig. 5d when porosity $\varphi < 0.165$, coefficient β falls rapidly instead, this is because a negative β occurs). However, in the course of loading, due to the crushing of edges and corners and the adjustment of the structure, the pore channels become more uncertain; as a result, both the $k - \varphi$ and $\beta - \varphi$ curves display some local fluctuation.

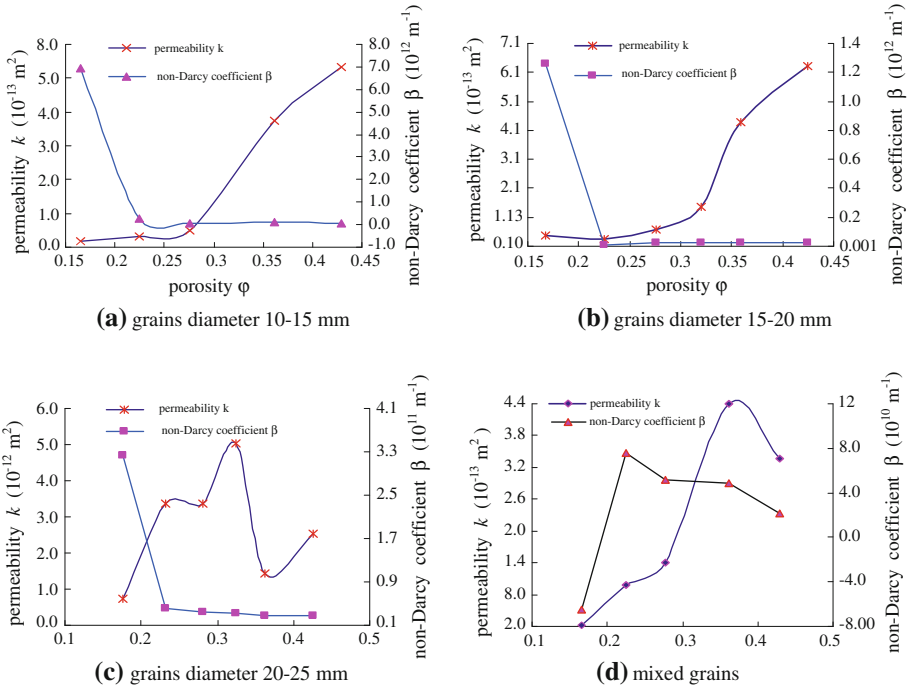

Fig. 5 $k-\varphi$ and $\beta-\varphi$ curves for sandstone of different grain sizes

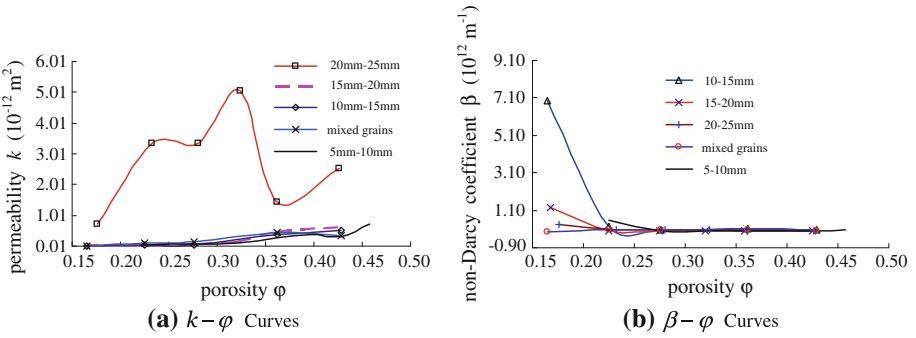

Fig. 6 Comparison of seepage properties for five sizes of broken sandstone

(3) The larger the grain diameter, the higher the permeability. For example, as shown in Fig. 6, the permeability of broken sandstone with a grain diameter of 20–25 mm is two orders of magnitude greater than that of broken sandstone with a grain diameter of 5–10 mm, while the non-Darcy coefficient β is one to two orders smaller.

(4) In Fig. 5c the fluctuations of $k-\varphi$ are especially intense compared with the other figures and the permeability shows a maximum at a porosity less than the initial porosity. In all our experiments a grain diameter 20–25 mm is the biggest size and the uniformity of its initial pore distribution is relatively poor compared with the other grain sizes. If the initial pore is not conducive to forming effective seepage channels, its permeability corresponding to initial big porosity is less instead than that at a low porosity. While at

the middle stage of loading, the decrease in porosity is possibly due to the breaking of grains and reconstructing of porous structure. If this porous structure results in more effective seepage passages then even if the porosity is less than the initial porosity the permeability is greater. In a word, the seepage properties of broken sandstone are not only related to loading levels but also to grain diameters, style of arrangement, and the initial pore structure (such as the initial pore channel).

(5) According to our experimental results, the magnitude of k and β for the broken sandstone ranges from 10^{-14} to 10^{-12} m^2 and from 10^{10} to 10^{12} m^{-1}, respectively. In some experiments, the coefficient β became negative when the permeability decreased to 10^{-14} m^2. Possible reasons for this phenomenon are as follows: (a) when the grains are compacted to break strongly and the seepage resistance through the felt is large, the calculation of the pore pressure gradient at the two ends of the sample with Eq. 8 may lack accuracy; (b) when the axial displacement is large, the crushing of grains becomes so serious that the relation between the pore pressure gradient and flow velocity is not nearly as simple as suggested by Eq. 6; (c) the thickness of the felt influences the pressure gradient between the two ends of the sample; (d) the method of calculating k and β by curves regression may have introduced some accumulative errors.

5 Conclusions

Given our loading method of controlling axial displacements and steady seepage, the seepage properties of broken sandstone have been studied. We have presented the results of our seepage experiment under different conditions of porosity. Our main conclusions are as follows:

(1) The relation of pore pressure gradient and flow velocity can be fitted by the quadratic Forchheimer equation, i.e., the flow in broken rock is a non-Darcy flow.
(2) In general, with a decrease in porosityφ, the permeability k decreases and the absolute value of the non-Darcy coefficient β increases, but both the $k-\varphi$ and $\beta-\varphi$ curves display local fluctuations; the greater the grain diameter, the more the fluctuation is displayed in the curves.
(3) The seepage properties of broken sandstone are not only related to loading levels but also to grain diameters, style of arrangement, and the initial pore structure (such as the initial pore channel).
(4) The magnitudes of k and βobtained from the experiments are 10^{-14}–10^{-12} m^2 and 10^{10}–10^{12} m^{-1}, respectively.

Acknowledgments The authors gratefully acknowledge the financial support from the National Basic Research Program of China (Project No. 2007CB209400) and the National Natural Science Foundation of China (Project No. 50634050, 50974107, and 50974115)

References

Bear, J.: Dynamics of Fluid in Porous Media. Dover, New York (1979)
Engelhardt, I., Finsterle, S.: Thermal-hydraulic experiments with bentonite/crushed rock mixtures and estimation of effective parameters by inverse modeling. Appl. Clay Sci. **23**(1), 111–120 (2003)
Giorgi, T.: Derivation of the Forchheimer law via matched asymptotic expansions. Transp. Porous Media **29**, 191–206 (1997)

Irmay, S.: On the theoretical derivation of Darcy and Forchheimer formulas. J. Geophys. Res. **39**(4), 702–707 (1958)
Kogure, K.: Experimental study on permeability of crushed rock. Mem. Def. Acad. Jpn. **16**(4), 149–154 (1976)
Kong X.: Advanced Mechanics of Fluid in Porous Media. Press of China University of science and technology, Hefei (1999) (in Chinese)
Legrand, J.: Revisited analysis of pressure drop in flow through crushed rocks. J. Hydraulic Eng. **128**(11), 1027–1031 (2002)
Li, S.: Nonlinear Dynamical Study on Non-Darcy Flow in Broken Rock. China University of Mining and Technology, Xuzhou (2006) (in Chinese)
Li, B., Garga, V.K., Davies, M.H.: Relationships for non-Darcy flow in rock fill. J. Hydraulic Eng. **124**(2), 206–211 (1998)
Liu, W.: Study on Theory and Application of Seepage in Overbroken Rock Mass. PhD Dissertation. China University of Mining and Technology, Beijing (2002) (in Chinese)
Liu, W., Miao, X.: A testing method for determining the permeability of overbroken rock. J. Exp. Mech. **18**(1), 57–61 (in Chinese) (2003)
Ma, Z.: Studies on Characteristics of Water Seepage in Overbroken Rock Mass of Gob. Xuzhou, China University of Mining and Technology (2003) (in Chinese)
McCorquodale, J.A., Hannoura, A-A.A., Nasser, M.S.: Hydraulic conductivity of rock fills. J. Hydraulic Res. **16**(2), 123–137 (1978)
Pradip Kumar, G.N., Venkataraman, P.: Non-Darcy converging flow through coarse granular media. J. Inst. Eng. (India): Civil Eng. Div. **76**, 6–11 (1995)
Stephson, D.: Hydraulic Calculation in Rock fills Engineering. Ocean Publishing Company, Beijing (1984)
Wang, M.L., Miao, S., Maji, A.K.: Deformation mechanisms of WIPP backfill. Radioactive Waste Manag. Environ. Restor. **20**(2), 191–211 (1996)
Zoback, M.D., Byerlee, J.D.: Note on the deformational behavior and permeability of crushed granite. Int. J. Rock Mech. Min. Sci. Geomech. Abstr. **13**(10), 291–294 (1976)